



# Preparation and modification of PVDF membrane via VIPS method for membrane distillation

Zhen Li<sup>1</sup> · Jianbing Wang<sup>1</sup> · Shuqin Liu<sup>1</sup> · Jingfeng Li<sup>2</sup>

Received: 26 December 2023 / Accepted: 16 April 2024 / Published online: 13 May 2024  
© The Author(s) 2024

## Abstract

Membrane distillation (MD) is a promising technology for treating high-salinity mine water. However, MD membranes are known to have low membrane flux and are prone to fouling. In this study, we used the cost-effective and controllable vapor-induced phase separation (VIPS) technology to prepare polyvinylidene difluoride (PVDF) membranes, replacing the traditional immersion precipitation method and optimizing the membrane structure by including LiCl and acetone as porogen in the casting solution. The results showed that the membrane prepared using the VIPS method exhibited a highly open interconnected porous surface. Unlike traditional MD membranes with a dense epidermal layer and large finger-like pores, these optimized membranes had a symmetrical and uniform internal structure, leading to a high flux of  $8.62 \text{ kg}\cdot(\text{m}^2\cdot\text{h})^{-1}$  during direct contact membrane distillation testing. Different porogens produced varied results on the VIPS process and varying effects on membrane structure. The use of LiCl promoted the formation of PVDF  $\beta$ -phase, resulting in a decrease in the number of spherical nodules on the membrane surface, as well as improved density and smoothness. Consequently, this reduced fouling risk during membrane distillation while slightly decreasing membrane flux. On the other hand, acetone rapidly evaporated during the VIPS process, facilitating pre-gelatinization and  $\alpha$ -phase formation of PVDF. This concurrent effect effectively restricted excessive nodule growth on the membrane surface, endowing the membrane with antifouling capabilities while preserving high flux.

**Keywords** Membrane distillation · Vapor-induced phase separation · Polyvinylidene fluoride membranes · Porogen · LiCl

## Introduction

Coal mining activities generate a large amount of high-mineralized mine water, which if untreated and directly discharged, could lead to resource waste and surrounding environmental pollution (Banks et al. 1997; Janson et al. 2009). In comparison with conventional mine water treatment methods, membrane distillation (MD) stands out as a novel membrane-based treatment option that capitalizes on material volatility. MD comes with several advantages over traditional practices, such as a high retention rate, low

operating pressure, small equipment volume, and ease of integration with other technologies (Alkudhiri et al. 2012). Additionally, MD technology can be powered by local solar or geothermal energy resources, providing an opportunity to reduce the energy consumption and cost of mine water treatment, making it highly applicable in mine water treatment. Despite these advantages, the limited membrane flux, severe membrane fouling, and wetting issues during operation have impeded the industrial application of membrane distillation technology (Chang et al. 2021; Li et al. 2019; Yao et al. 2020).

Membrane materials and their preparation processes play a crucial role in determining the performance and application outcomes of membrane distillation technology. Polyvinylidene fluoride (PVDF) is a highly sought-after membrane material in membrane distillation fields due to its high hydrophobicity, exceptional chemical stability, thermal stability, contamination resistance, and mechanical properties (Liu et al. 2011). Currently, the most extensively adopted industrial approach to prepare PVDF membranes is

✉ Zhen Li  
chestnutbean@foxmail.com

<sup>1</sup> School of Chemical and Environmental Engineering, China University of Mining and Technology (Beijing), D11 Xueyuan Road, Haidian District, Beijing 100083, China

<sup>2</sup> State Key Laboratory of Water Resource Protection and Utilization in Coal Mining, China Energy Investment Corporation, Beijing 100011, China

immersion precipitation. In this method, phase separation is achieved by immersing the polymer solution in a non-solvent bath. However, despite its popularity, PVDF membranes prepared using this technique frequently feature a dense skin layer on the surface, which significantly hampers their membrane flux during membrane distillation. Furthermore, the rapid rate of phase separation characteristic of the immersion precipitation method can contribute to the formation of a macroscopic finger-like pore structure within the membrane, ultimately compromising its mechanical stability (Thomas et al. 2014).

Vapor-induced phase separation (VIPS) is a technology that utilizes non-solvent vapors to initiate phase separation between solvents and polymers. In this process, the gas-phase infiltration of the non-solvent into the casting solution system results in a gradual and more controllable absorption by the system (Lee et al. 2004; Li et al. 2010; Su et al. 2009; Tsai et al. 2010). This controlled absorption, compared to the slower evaporation rate of low-volatile solvents during VIPS, leads to a lower polymer concentration in the surface region of the membrane (Su et al. 2009). This, in turn, fosters the creation of porous surfaces, rendering VIPS technology distinctive in the realm of fabricating MD (microfiltration and ultrafiltration) membranes. The unique characteristics of VIPS facilitate the preparation of membranes with desirable properties, with the outcomes and findings presented in the past tense (Fan et al. 2013; Peng et al. 2013).

Over the years, researchers have dedicated themselves to enhancing the membrane structure and performance by fine-tuning the VIPS process parameters. Su et al. (2009) found that the membrane pores of VIPS membranes coarsen from a bi-continuous structure to a cellular structure with increasing exposure time. Zhao et al. (2018) fabricated membranes with cellular structure and improved the mechanical strength of the membranes by modulating the effects of parameters such as vapor temperature and exposure time during the VIPS process. Venault et al. (2023) also increased the contact angle of the PVDF film and improved its wettability in MD by adjusting the VIPS process parameters. However, the improvement brought by process optimization is relatively limited. In immersion precipitation, the introduction of non-solvent additives into the casting system has been widely used as a simple and effective way of improving membrane properties. Indeed, some studies have found that the introduction of additional additives into the VIPS casting solution can lead to changes in membrane performance. Sun et al. (2007) found that adding glycerol as a non-solvent in the VIPS method for the preparation of nitrocellulose microfiltration membranes increased the porosity and pure water flux of the membrane, thereby improving the pore structure. Susanto et al. (2009) discovered that in the preparation of polyethersulfone microfiltration membranes, two additives, amphiphilic PEG block copolymer, and

TEG enhanced the hydraulic permeability of the VIPS process, thereby improving the membrane. Unfortunately, using porogens in the VIPS process is limited and not well-researched.

LiCl is a common immersion-precipitated pore-making agent, which, as an aqueous salt, can be easily removed from the membrane by the immersion process (Chakrabandhu et al. 2008; Meng et al. 2017; Venault et al. 2014; Ye et al. 2011; Yushkin et al. 2022). Wang et al. (2000) achieved PVDF membranes with high mechanical strength and gas permeability by incorporating a small amount of LiCl additive in immersion precipitation. Similarly, Devi et al. (2009) reported that the inclusion of LiCl, as a porogen in the casting solution of CA/SiO<sub>2</sub> blended ultrafiltration membrane, enhances the membrane's permeation flux. However, the application of LiCl in VIPS technology seems to have been rarely studied. In addition to LiCl, acetone is also a common porogen (Moghadassi et al. 2017), but it is more volatile, which will be highlighted in the VIPS process. Hence, it remains unclear whether the volatilization of pore-forming agents would bring different impacts to the VIPS process, raising an exciting question.

Therefore, in this study, acetone and LiCl were selected as representatives of volatile and nonvolatile porogen, and they were blended separately in the casting solution to prepare PVDF membranes using the VIPS method. This study discussed the effects of these porogens on the membranes' morphology, pore structure, physicochemical properties, and their mechanism of influence on the phase transition during the VIPS process. Additionally, the influence of these changes on the membrane distillation performance of the membranes was also analyzed. Such a study will not only help us to understand these additives more deeply and provide a reference for the selection of porogens for the VIPS method. It also provides a research basis for more porogens with similar principles of action for VIPS applications and helps to expand the number of porogens suitable for VIPS.

## Experimental section

### Materials and reagents

Polyvinylidene fluoride (PVDF) was purchased from Shanghai Huayi 3F New Materials Co., Ltd; N-methyl pyrrolidone (NMP), analytical pure, from US MREDA reagent; acetone, analytically pure, Sinopharm Chemical Reagent Co., Ltd; anhydrous lithium chloride, high-purity reagent, TCI (Shanghai) chemicals; nonwoven support layer TA3631, Shanghai Tianlue Textile New Material Co., Ltd; sodium chloride, analytical pure, Shanghai Yuanye Biotechnology Co., Ltd; adjustable film applicator, BEVS

1806b/100, BEVS Industrial (Guangzhou) Co., Ltd.; thermostatic-humidistat cultivating box, hws-50b, Shanghai Qiuzuo Scientific Instrument Co., Ltd; deionized water, self-made, with conductivity less than 5  $\mu\text{s}/\text{cm}$ .

## Membrane preparation

Dissolve PVDF powder at a concentration of 12wt % in NMP, followed by the addition of 4wt % LiCl, 4wt % acetone, or no additive concerning the solution mass. During the dissolution process, keep the temperature at 65 °C and constantly stir until the solution is completely uniform. The stirred film-forming solution should be used after standing for defoaming.

Apply the casting solution onto the nonwoven substrate using an adjustable film applicator. Place the scraped film in a vacuum oven at 40 °C for 5 min, and then transfer it to a thermostatic-humidistat cultivating box with a temperature of 40 °C and a relative humidity of 68% RH, where the film is exposed to water vapor for 15 min. Then immerse the VIPS-treated membrane in deionized water for 24 h to remove residual solvents. Finally, the film is naturally dried at room temperature for use (Fig. 1). The membranes prepared using LiCl additive, acetone additive, and casting solution without any additive are labeled as M-LiCl, M-AC, and M-0, respectively.

## Characterization

The surface morphology of the film was observed using a Thermo Scientific Phenom Pharos field emission scanning electron microscope at a voltage of 15 kV. Before the surface observation, the PVDF surface was subjected to surface sputtering with gold using a Quorum SC7620 sputter coating machine for 45 s. For sectional analysis, the film was first immersed in liquid nitrogen to achieve neat brittle fracture, and then the same steps were followed to spray gold. Finally,

the cross-sectional morphology was observed using the Czech TESCAN MIRA LMS scanning electron microscope. The roughness of the membrane surface was measured using an atomic force microscope (AFM, Bruker Dimension Icon, USA), with a single scan area size of 15  $\mu\text{m}$ \*15  $\mu\text{m}$ . The surface elements of the membrane were detected using the energy-dispersive spectroscopy (EDS) detector attached to the SEM system, and the characteristic functional groups on the membrane surface were detected using a Fourier transform infrared spectrometer (FTIR, PerkinElmer, USA) in the total reflection (ATR) mode with a wave number range of 400–4000  $\text{cm}^{-1}$ . Use ImageJ software to measure the porosity and pore size of the membrane surface, statistically calculate the average pore size and pore size distribution, and statistically analyze at least 200 pore size values for each membrane group. The instantaneous static contact angle of the film surface was measured at room temperature using a goniometer/tension meter (ramé-hart MODEL250, USA), and the results were averaged from three measurements. The liquid used for the measurement is deionized water.

## DCMD setup and experiments

The direct contact membrane distillation (DCMD) device is from Shanghai Tongqin Technology Co., Ltd. The schematic diagram of the device structure is shown in Fig. 2. The device adds an automatic recording unit module and uses a low-temperature thermostat and a low-temperature thermostat for temperature control. The effective area of the flat membrane module is 32  $\text{cm}^2$ . The feed side uses simulated concentrated brine with a concentration of 3.5 wt % NaCl as the feed solution, while the condensate side uses deionized water as the circulating water. Both sides are circulated by a peristaltic pump, with a circulating flow rate of 18 L/h. The feed liquid temperature is maintained at 55 °C, and the permeate side temperature is maintained at 20 °C. The changes

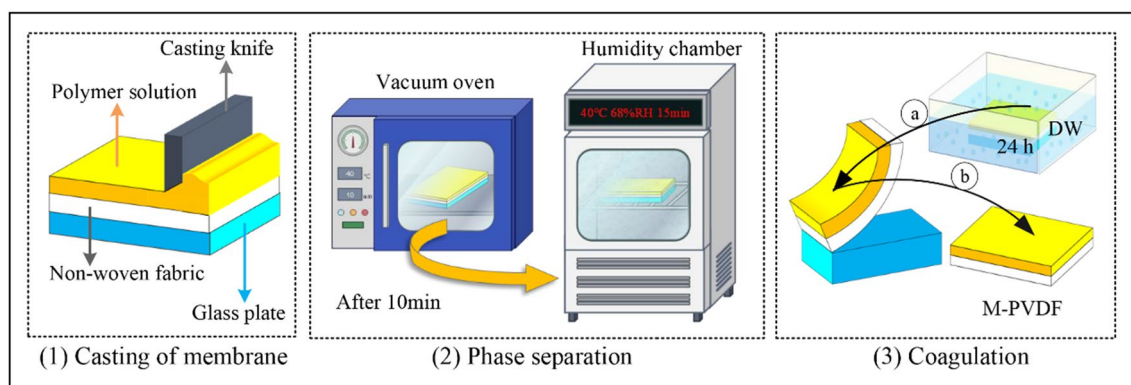
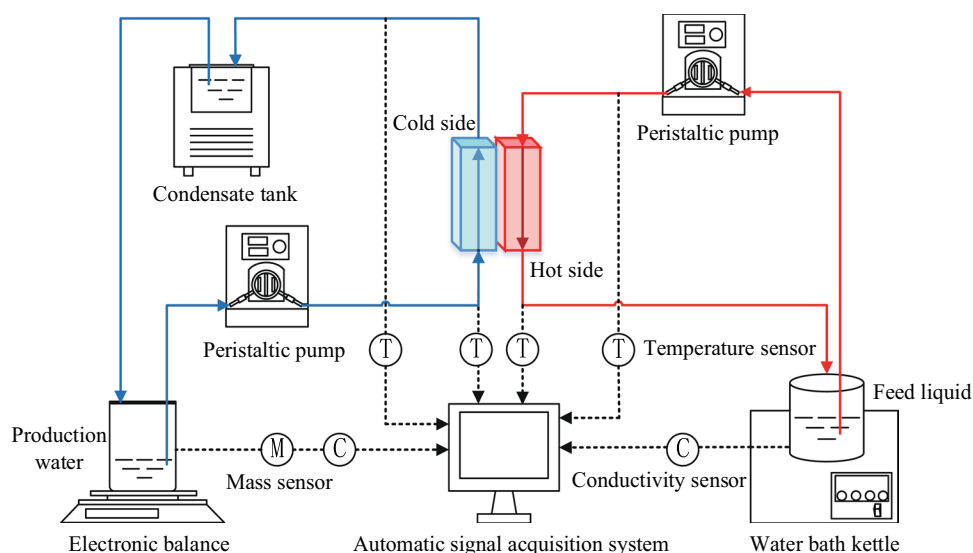


**Fig. 1** Process flow of preparing PVDF membrane by VIPS method

**Fig. 2** Schematic diagram of DCMD device structure



in the mass and conductivity of the permeate are recorded every 5 min.

The permeation flux of the membrane is calculated by the following equation:

$$J = \frac{m}{A \cdot t} \quad (1)$$

where  $J$  represents membrane flux ( $\text{kg} \cdot \text{m}^{-2} \text{h}^{-1}$ ),  $m$  is the change in mass of the permeate measured (kg),  $A$  represents effective membrane area ( $\text{m}^2$ ), and  $t$  represents sampling interval (h).

The rejection rate of the membrane is calculated by Eq. (2):

$$R = \left(1 - \frac{C_p}{C_f}\right) \times 100\% \quad (2)$$

$R$  represents the retention rate of the membrane, where  $C_p$  and  $C_f$  are, respectively, the permeate and the feed concentrations.

## Results and discussion

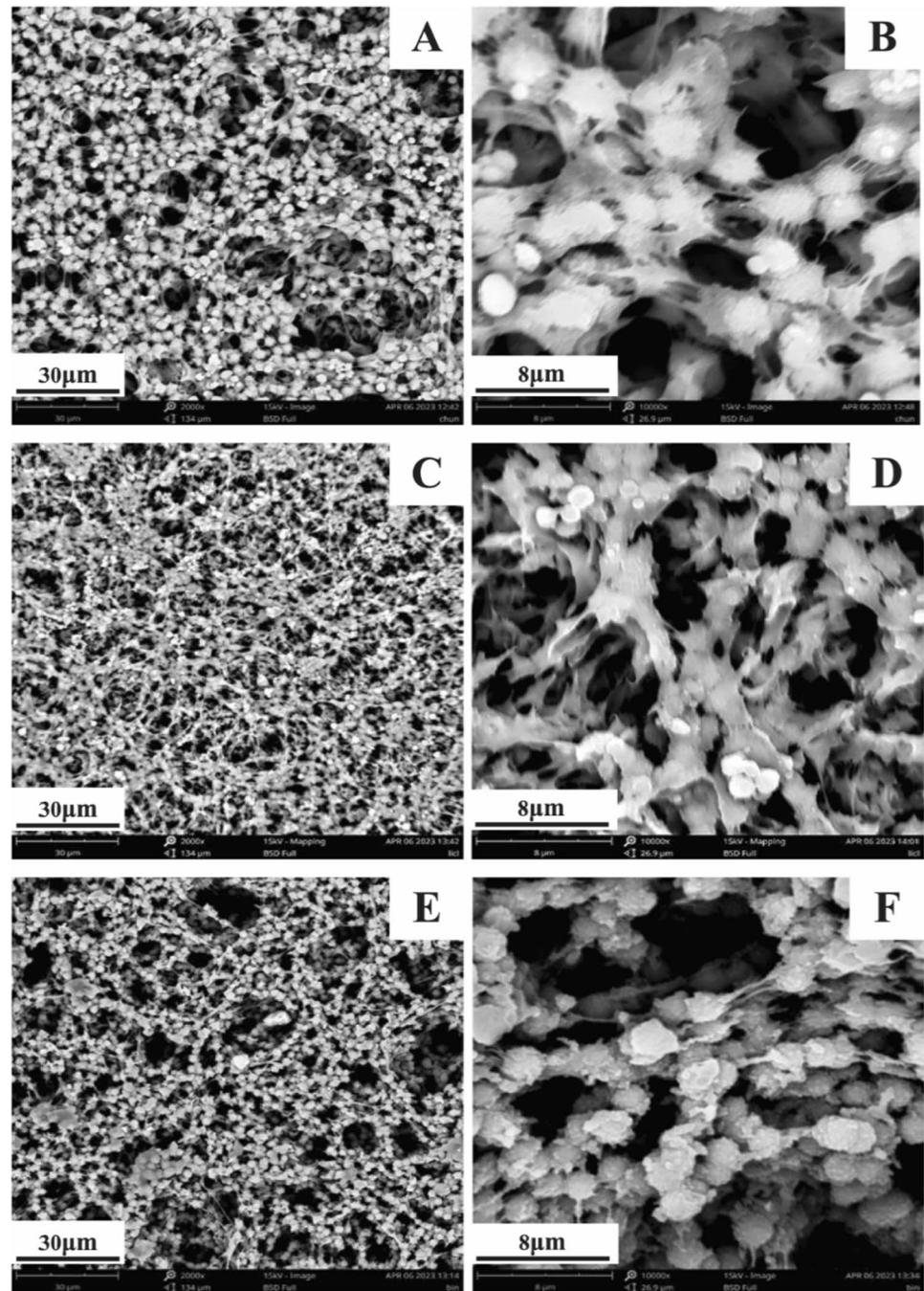
### Effect of additives on the morphology of PVDF membrane

The surface of PVDF membranes prepared by the VIPS method exhibits a highly open and interconnected porous surface structure, rather than a dense skin layer like traditional NIPS membranes, as can be seen from the surface SEM image of the membrane (Fig. 3). Compared to the film without additives, the effects of the two additives on the surface morphology of the film showed completely opposite trends: For the film with LiCl added, the PVDF nodules

(spheroids) on the surface decreased and the connectivity increased, while the surface nodules increased and the continuous structure further decreased for the film with acetone added. The formation of nodular structures is often related to gelation induced by crystallization (Su et al. 2009): PVDF crystals undergo pre-gelation before phase separation, and the presence of colloidal particles provides active sites conducive to nucleation, while also increasing local polymer concentration, promoting the formation of crystalline nuclei, accelerating the growth process of crystallization, and ultimately forming nodular structures. The addition of LiCl will increase the viscosity of the polymer solution and increase the diffusion resistance of the polymer chain, which will have a certain adverse effect on the process of PVDF pre-gelation. Due to its strong volatility, acetone will be largely extracted from the solvent during the VIPS process, which is beneficial for the pre-gelation of PVDF, which explains why the film with acetone added will have more nodular structures.

From the cross-sectional images of the membranes (Fig. 4), it can be seen that the membranes prepared by the three VIPS methods all exhibit a relatively symmetric membrane structure, without macroscopic finger-like pore structures. Both the unadded and LiCl-added membranes exhibit a bi-continuous (lacy) structure, while the membrane with acetone exhibits a typical cell structure. Polymer solutions can undergo phase separation through two mechanisms: nucleation and growth mechanisms and spinodal decomposition. The bi-continuous structure is generally formed by spinodal decomposition, while the cellular structure is generally formed by nucleation and growth mechanisms. Theoretically, the longer the polymer solution stays in the metastable region, the higher the probability of the solution phase separating through nucleation and growth mechanisms. In other words, the shorter the time in the metastable

**Fig. 3** SEM pictures of the membranes. **A, B** M-0, **C, D** M-LiCl, and **E, F** M-AC

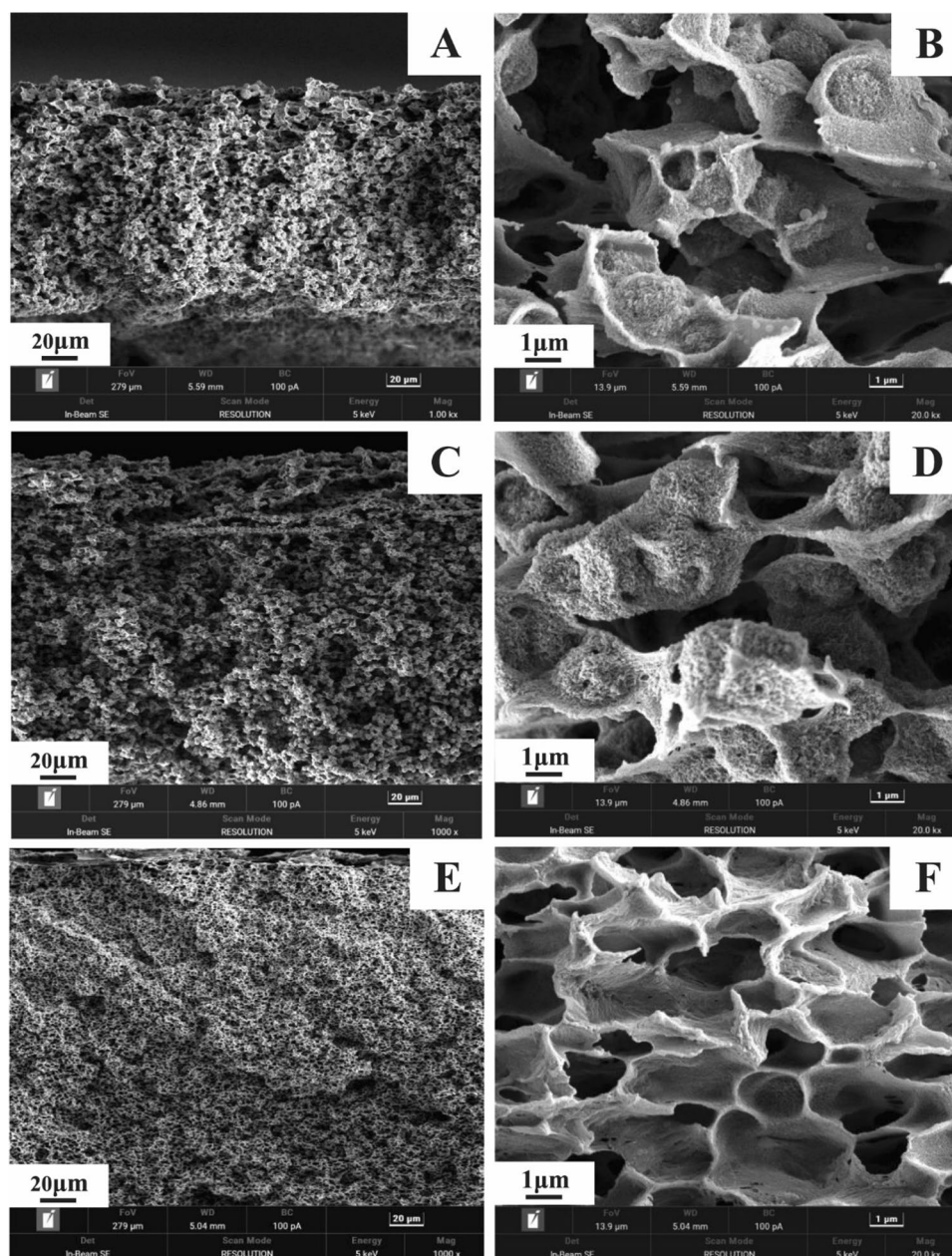


region, the more likely it is that the polymer solution will pass through the metastable region without phase separation and undergo spinodal decomposition in the unstable region (Desmet et al. 2017; Su et al. 2009). For solvents with acetone added, the pre-gelation of PVDF forms a "skin layer" on the membrane surface, blocking the further intrusion of water vapor, allowing sufficient time for the solution inside the membrane to remain in the metastable region, promoting the nucleation and growth mechanism of the solution, and

enabling the internal membrane to acquire a more distinct cellular structure.

Figure 5 shows the AFM image of the membrane surface, with dark areas representing "valleys" and light areas representing "peaks." It can be seen that the surfaces of the three membranes are covered with numerous undulating structures, resulting in high surface roughness, which increases the membrane surface contact angle and achieves high hydrophobicity. The film with LiCl added ( $R_a = 638$  nm) has a lower surface roughness compared

**Fig. 4** SEM pictures of the cross section of membranes. **A**, **B** M-0, **C**, **D** M-LiCl, and **E**, **F** M-AC



to the film without LiCl added ( $R_a = 891$  nm) due to the reduction of PVDF nodular structures on the surface. Interestingly, the film with acetone added also achieved a smoother surface ( $R_a = 595$  nm). Although adding acetone can result in more nodular structures in the membrane, it can also be seen from the SEM images that the nodular size of the membrane has been significantly reduced after adding acetone compared to the absence of acetone. This is due to the rapid evaporation of the solvent, which limits the further growth of the crystalline domains, resulting in smaller-sized microcrystals, and therefore a smoother film.

### Effect of additives on the pore size distribution of PVDF membranes

The porosity, average pore size, and pore size distribution of the membrane surface measured using ImageJ software are shown in Table 1 and Fig. 6.

Compared to M-0, the average pore size and porosity of the M-LiCl membrane have slightly increased, possibly due to the fact that LiCl acts as a swelling agent, increasing the viscosity of the PVDF solution. The increase in solution viscosity can slow down the pore formation process and reduce

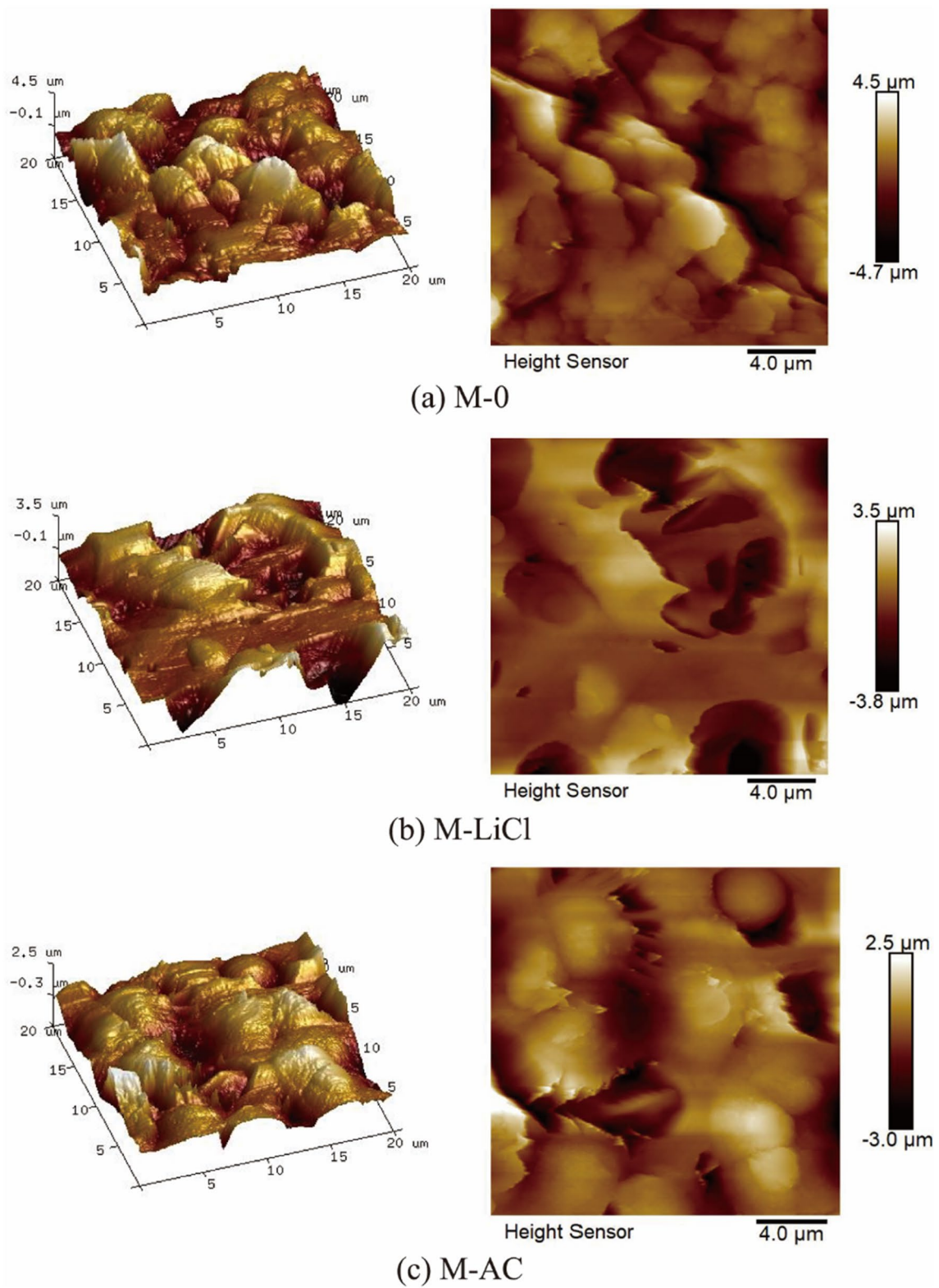


Fig. 5 AFM diagrams of three types of PVDF membranes

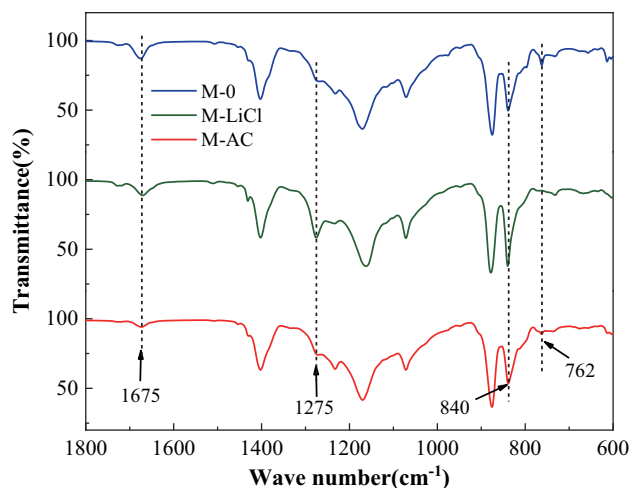
**Table 1** Porosity and average pore size of three types of PVDF membranes

	M-0	M-LiCl	M-AC
Porosity/%	44.76	45.81	50.61
Average pore size/ $\mu\text{m}$	4.33	4.35	5.53

the phase separation rate, resulting in the formation of more pore structures and larger pore sizes. At the same time, the addition of LiCl can enhance the interaction between the PVDF polymer chain and the solvent, thereby improving the orderliness of the polymer chain in the solution, resulting in a more uniform pore size and a significantly narrower pore size distribution.

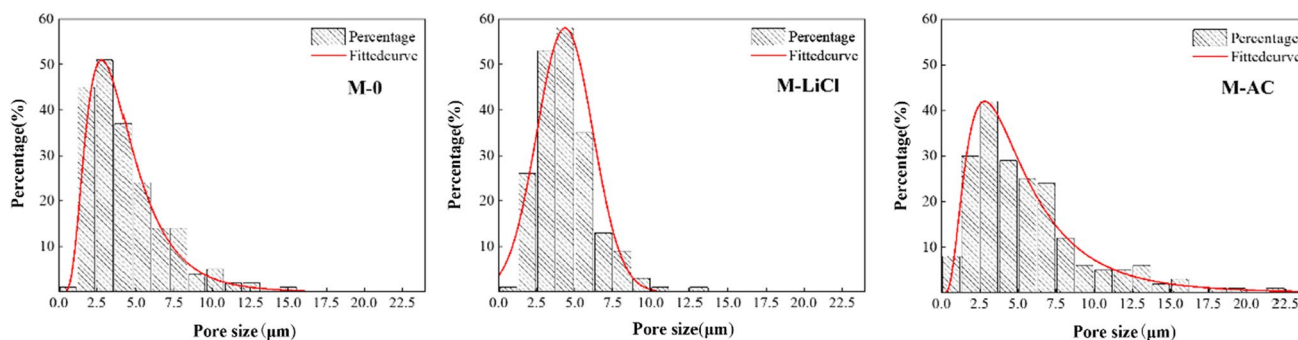
### The effect of additives on the chemical composition and hydrophobicity of PVDF membranes

To investigate the impact of additives on the chemical structure of the membrane, FTIR analysis was performed on the surfaces of all three membranes (Fig. 7). It can be seen that the absorption peaks of the three membranes are basically the same, indicating that the addition of acetone and LiCl does not affect the basic chemical structure of PVDF. However, the signal intensity of the peaks at  $762\text{ cm}^{-1}$ ,  $840\text{ cm}^{-1}$ , and  $1275\text{ cm}^{-1}$  on the infrared spectrograms of the three membranes changed significantly. These peaks in the fingerprint region signify subtle changes in PVDF conformation,  $840\text{ cm}^{-1}$  and  $1275\text{ cm}^{-1}$  correspond to the  $\alpha$ -phase of PVDF, while  $762\text{ cm}^{-1}$  corresponds to the  $\beta$ -phase. The changes in peak intensity suggest a shift in the main crystalline form of PVDF in the membrane. For M-LiCl, the peak signal at  $840\text{ cm}^{-1}$  and  $1275\text{ cm}^{-1}$  is significantly stronger than the other two membranes, while it is significantly weaker at  $762\text{ cm}^{-1}$ . This indicates that the main crystalline form of PVDF in M-LiCl is  $\beta$ -form, while the other two membranes have more  $\alpha$ -form. The PVDF chain of  $\beta$ -form is in the TTTT all-trans conformation, compared to  $\alpha$ -form

**Fig. 7** Fourier-infrared spectrum of membrane surface

has higher crystallinity and a tighter lattice structure, resulting in a more uniform pore structure and narrower pore size distribution in the film, consistent with the results presented in the SEM images. It is worth noting that at  $1675\text{ cm}^{-1}$ , the peak signal of M-AC is significantly weakened, which is not an inherent characteristic peak of PVDF but a characteristic peak of hydrogen bonding. The weakening of the peak signal may be due to the polarity of acetone, which causes a certain degree of interaction with PVDF, thereby affecting the hydrogen bonding between PVDF molecular chains.

The distribution of elements on the surface of the membrane was detected using EDS spectroscopy (Fig. 8). The surface of the three membranes is still dominated by C and F elements, indicating that the two additives are not likely to remain in the membrane. Trace amounts of residual Cl elements were detected on the surface of the membrane with LiCl added, while oxygen elements representing residual acetone were not detected on the surface of the membrane with acetone added due to the high volatility of acetone. In addition, from the surface scanning results, both the surfaces of the films without acetone and those with acetone

**Fig. 6** Pore size distribution of three types of PVDF membranes



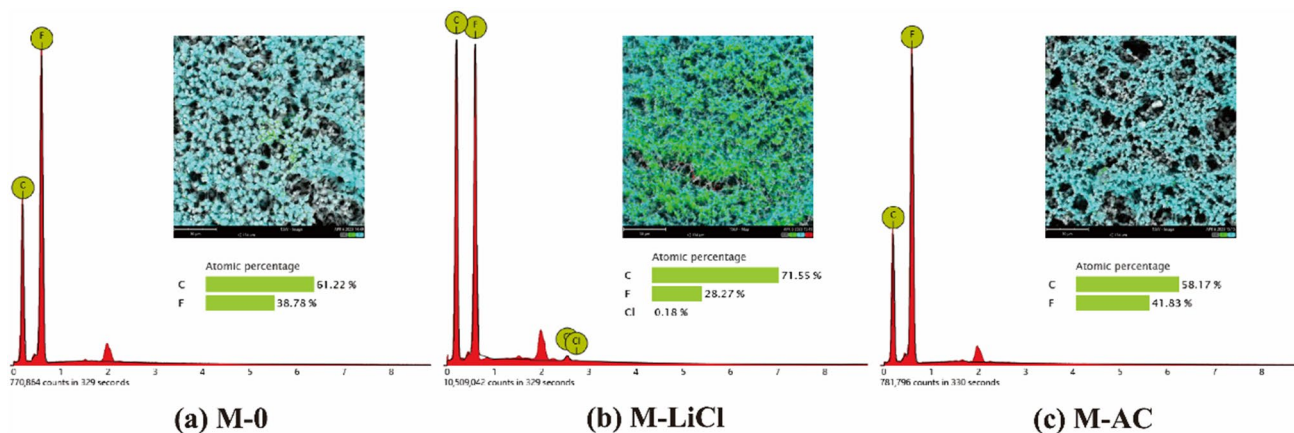


Fig. 8 EDS spectrum results of the membrane surface

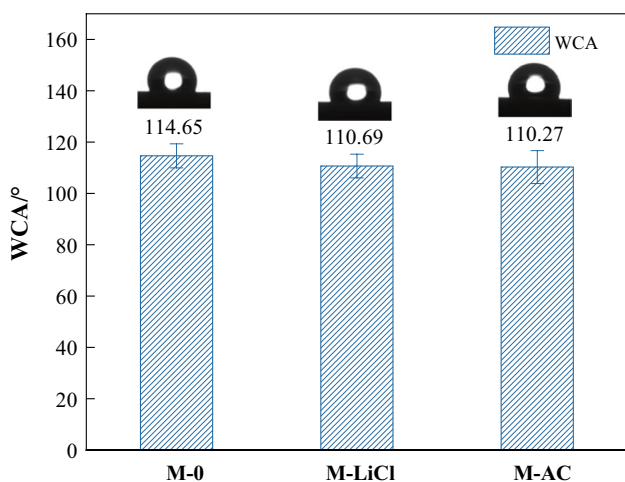


Fig. 9 Water contact angle values of three PVDF membrane surfaces

have a relatively high fluorine-to-carbon ratio, which may be related to the fact that both films have a relatively loose PVDF nodular structure, which increases the exposure of F atoms on the surface and thus increases the fluorine-to-carbon ratio.

The hydrophobicity of the membrane is also an important parameter for membrane distillation membranes. The contact angle of water on the membrane surface is measured using a contact angle meter to evaluate the hydrophobicity of the membrane (Fig. 9). The three membrane surfaces all achieved high contact angles (> 110°), which is related to the high hydrophobicity of PVDF material itself and the loose and porous surface structure of the membranes prepared by the VIPS method. At the same time, we were surprised to find that even though both additives are polar hydrophilic and both significantly reduce the roughness of the membrane surface, which theoretically would reduce the hydrophobicity of the membrane, the hydrophobicity angle of the

membrane did not suffer significantly. This may be because both additives are essentially not retained in the membrane, and their improvement of the membrane structure to some extent offsets the impact of the decrease in roughness, allowing the membrane containing the additive to maintain a high contact angle.

### DCMD performance

Using 3.5 wt% NaCl as simulated water, the membrane distillation performance of three membranes was tested using a DCMD device. Figure 10 shows the changes in flux and rejection rate of three PVDF membranes during the actual 6-h operation of membrane distillation.

At the initial stage of operation, both M-0 and M-AC have high fluxes,  $8.62 \text{ kg}\cdot(\text{m}^2\cdot\text{h})^{-1}$  and  $8.31 \text{ kg}\cdot(\text{m}^2\cdot\text{h})^{-1}$ , respectively, while the flux level of M-LiCl is relatively low, at  $5.89 \text{ kg}\cdot(\text{m}^2\cdot\text{h})^{-1}$ , which may be due to the relatively dense membrane structure of the membrane with added LiCl. With the operation of MD, the flux of M-0 began to decline significantly from 3 h, and by the end of the operation, the flux had dropped to 54.06% of the initial flux. This may be due to the high roughness of the surface of M-0, which brings a high contact angle, but the rough surface also increases the risk of inorganic matter crystallizing and depositing on the membrane surface, making it unable to maintain a high flux. Soon, membrane pollution occurred, leading to a significant decrease in membrane flux. However, the membrane with additives has a smoother surface due to the improvement of the membrane structure by the additives, which enhances its antifouling ability and allows its membrane flux to remain at a relatively stable level during testing.

From the changes in rejection rate (Fig. 10b), all three membranes achieved a rejection rate of 99.9% or higher at the beginning, indicating that the membranes prepared

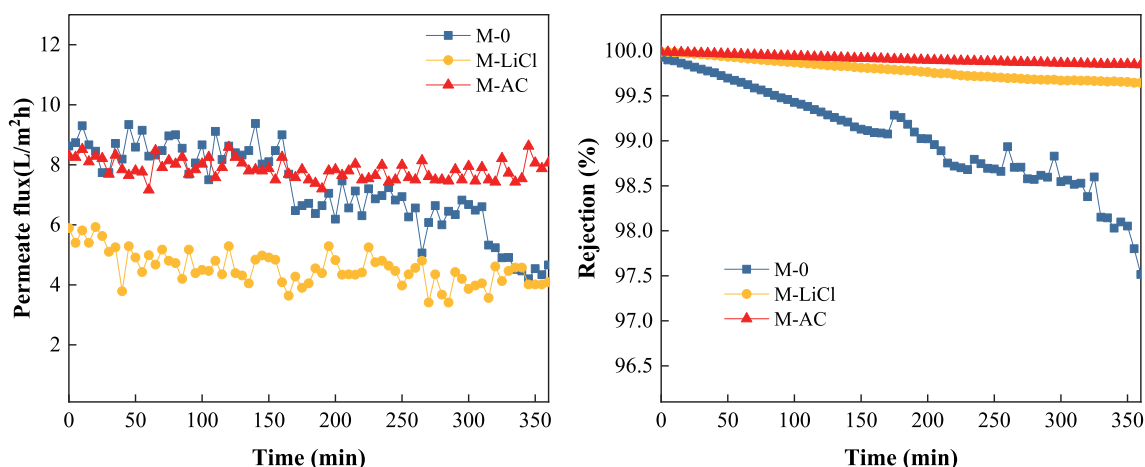


**Fig. 10** MD performance test of membrane **a** membrane flux **b** rejection

using VIPS exhibit excellent rejection performance in MD. During the operation process, the retention rate of the membrane with additives remained stable, especially for M-AC, which remained above 99.9% throughout the entire test. However, the rejection rate of the membrane without added materials showed a significant decline. Although the final rejection rate remained above 97%, it did not perform well compared to the other two membranes, which consistently maintained a high rejection rate of over 99.5%. The decrease in the rejection rate of the M-0 membrane may be related to the occurrence of wetting phenomena. Due to membrane fouling, NaCl crystals are deposited on the membrane surface and pores, providing water channels for liquid transport, resulting in a decrease in rejection rate.

A comprehensive comparison of the performance of the three membranes showed that both the addition of acetone and LiCl can improve the membrane distillation performance, reduce the risk of membrane fouling, and provide a relatively stable level of membrane flux and rejection during service. In addition, using acetone as an additive can maintain a high membrane flux, achieving the best performance in the MD test.

## Conclusion

Acetone and LiCl are representative of volatile additives and thickening additives. They were blended separately in the casting solution and prepared PVDF membranes using the VIPS method. Through the study of the structure of the membrane and the distillation performance of the membrane, the following conclusions were obtained:

- (1) Adding LiCl to the casting solution increases the viscosity of the solution, hinders the pre-gelation of PVDF before phase separation, produces more  $\beta$ -crystalline form of PVDF increases the continuity of the membrane surface structure, reduces nodular structures, and reduces roughness. The membrane exhibits a more uniform pore structure and narrower pore size distribution.
- (2) Acetone has high volatility and polarity, when added to the casting solution, it promotes the pre-gelation of PVDF, resulting in more surface nodules, and the film tends to produce more  $\alpha$ -form. The film exhibits a looser surface structure and wider pore size distribution, and the porosity and pore size of the film surface also have a significant increase. At the same time, the rapid evaporation of the solvent restricts further crystal growth, resulting in smaller-sized microcrystals, which makes the film smoother. Moreover, the pre-gelled skin layer prevents further invasion of non-solvent and promotes the formation of cell structures inside the film.
- (3) Both additives reduce the risk of membrane surface contamination and maintain relatively stable flux and retention rates during MD operation. However, the average flux of the membrane with LiCl addition is lower due to its dense surface structure; the membrane with acetone added exhibited higher flux and retention, achieving the best performance in the membrane distillation test run.

Our study reveals different effects of porogen with different pore-forming principles on membrane structure (e.g., the addition of LiCl results in more uniform membrane pores, whereas the addition of acetone increases the average pore size and membrane flux). Therefore, suitable additives

can be selected based on the desired structural direction to be controlled. Based on these two typical pore-forming additives, further research can be carried out in the future for more cost-effective or environmentally friendly additives that improve MD performance. This will help simplify the VIPS methodology and facilitate the industrial production of MD membranes.

**Acknowledgements** Thank Dr. Qi Chuan for his valuable advice in this manuscript.

**Author contributions** All authors contributed to the study conception and design. Conceptualization, formal analysis, methodology, visualization, and writing—original draft were performed by ZL. Data curation, project administration, resources, and validation were performed by Jianbing Wang. Supervision and writing—review and editing were performed by SL, and investigation was performed by JL. All authors read and approved the final manuscript.

**Funding** This work was supported by the National Natural Science Foundation of China (52270084); the Open Fund Project of the State Key Laboratory of Water Resources Protection and Utilization in Coal Mining (GJNY-18-73.13); and the China University of Mining and Technology (Beijing) Yue Qi outstanding scholar program (2020JCB02).

## Declarations

**Conflict of interest** The authors declare that they have no conflict of interest.

**Research involving human participants and/or animals** This article does not contain any studies with human participants performed by any of the authors.

**Informed consent** Informed consent was obtained from all individual participants included in the study.

**Open Access** This article is licensed under a Creative Commons Attribution 4.0 International License, which permits use, sharing, adaptation, distribution and reproduction in any medium or format, as long as you give appropriate credit to the original author(s) and the source, provide a link to the Creative Commons licence, and indicate if changes were made. The images or other third party material in this article are included in the article's Creative Commons licence, unless indicated otherwise in a credit line to the material. If material is not included in the article's Creative Commons licence and your intended use is not permitted by statutory regulation or exceeds the permitted use, you will need to obtain permission directly from the copyright holder. To view a copy of this licence, visit <http://creativecommons.org/licenses/by/4.0/>.

## References

- Alkhdhiri A, Darwish N, Hilal N (2012) Membrane distillation: a comprehensive review. *Desalination* 287:2–18. <https://doi.org/10.1016/j.desal.2011.08.027>
- Arthanareeswaran G, Devi TKS, Mohan D (2009) Development, characterization and separation performance of organic-inorganic membranes Part II. Effects of additives. *Sep Purif Technol* 67(3):271–281. <https://doi.org/10.1016/j.seppur.2009.03.037>
- Banks D, Younger PL, Arnesen R, Iversen ER, Banks SB (1997) Mine-water chemistry; the good, the bad and the ugly. *Environ Geol* 32(3):157–174. <https://doi.org/10.1007/s002540050204>
- Chakrabandhu Y, Pochat-Bohatier C, Vachoud L, Bouyer D, Desfours JP (2008) Control of elaboration process to form chitin-based membrane for biomedical applications. *Desalination* 233(1–3):120–128. <https://doi.org/10.1016/j.desal.2007.09.034>
- Chang H, Liu B, Zhang Z, Pawar R, Yan Z, Crittenden JC, Vidic RD (2021) A critical review of membrane wettability in membrane distillation from the perspective of interfacial interactions. *Environ Sci Technol* 55(3):1395–1418. <https://doi.org/10.1021/acs.est.0c05454>
- Desmet C, Valsesia A, Oddo A, Ceccone G, Spampinato V, Rossi F, Colpo P (2017) Characterisation of nanomaterial hydrophobicity using engineered surfaces. *J Nanopart Res*. <https://doi.org/10.1007/s11051-017-3804>
- Fan H, Peng Y, Li Z, Chen P, Jiang Q, Wang S (2013) Preparation and characterization of hydrophobic PVDF membranes by vapor-induced phase separation and application in vacuum membrane distillation. *J Polym Res*. <https://doi.org/10.1007/s10965-013-0134-4>
- Janson E, Gzyl G, Banks D (2009) The occurrence and quality of mine water in the upper Silesian Coal Basin, Poland. *Mine Water Environ* 28(3):232–244. <https://doi.org/10.1007/s10230-009-0079-3>
- Lee HJ, Jung B, Kang YS, Lee H (2004) Phase separation of polymer casting solution by nonsolvent vapor. *J Membrane Sci* 245(1–2):103–112. <https://doi.org/10.1016/j.memsci.2004.08.006>
- Li C, Wang D, Deratani A, Quemener D, Bouyer D, Lai J (2010) Insight into the preparation of poly(vinylidene fluoride) membranes by vapor-induced phase separation. *J Membrane Sci* 361(1–2):154–166. <https://doi.org/10.1016/j.memsci.2010.05.064>
- Li J, Guo S, Xu Z, Li J, Pan Z, Du Z, Cheng F (2019) Preparation of omniphobic PVDF membranes with silica nanoparticles for treating coking wastewater using direct contact membrane distillation: Electrostatic adsorption vs. chemical bonding. *J Membrane Sci* 574:349–357. <https://doi.org/10.1016/j.memsci.2018.12.079>
- Liu F, Hashim NA, Liu Y, Abed MRM, Li K (2011) Progress in the production and modification of PVDF membranes. *J Membrane Sci* 375(1–2):1–27. <https://doi.org/10.1016/j.memsci.2011.03.014>
- Meng J, Lin S, Xiong X (2017) Preparation of breathable and superhydrophobic coating film via spray coating in combination with vapor-induced phase separation. *Prog Org Coat* 107:29–36. <https://doi.org/10.1016/j.porgcoat.2017.03.004>
- Moghadassi AR, Bagheripour E, Hosseini SM (2017) Investigation of the effect of tetrahydrofuran and acetone as cosolvents in acrylonitrile-butadiene-styrene-based nanofiltration membranes. *J Appl Polym Sci*. <https://doi.org/10.1002/app.44993>
- Peng Y, Dong Y, Fan H, Chen P, Li Z, Jiang Q (2013) Preparation of polysulfone membranes via vapor-induced phase separation and simulation of direct-contact membrane distillation by measuring hydrophobic layer thickness. *Desalination* 316:53–66. <https://doi.org/10.1016/j.desal.2013.01.021>
- Su YS, Kuo CY, Wang DM, Lai JY, Deratani A, Pochat C, Bouyer D (2009) Interplay of mass transfer, phase separation, and membrane morphology in vapor-induced phase separation. *J Membrane Sci* 338(1–2):17–28. <https://doi.org/10.1016/j.memsci.2009.03.050>
- Sun H, Liu S, Ge B, Xing L, Chen H (2007) Cellulose nitrate membrane formation via phase separation induced by penetration of nonsolvent from vapor phase. *J Membrane Sci* 295(1–2):2–10. <https://doi.org/10.1016/j.memsci.2007.02.019>
- Susanto H, Stahra N, Ulbricht M (2009) High performance polyether-sulfone microfiltration membranes having high flux and stable hydrophilic property. *J Membrane Sci* 342(1–2):153–164. <https://doi.org/10.1016/j.memsci.2009.06.035>
- Thomas R, Guillen-Burrieza E, Arafat HA (2014) Pore structure control of PVDF membranes using a 2-stage coagulation bath phase

- inversion process for application in membrane distillation (MD). *J Membrane Sci* 452:470–480. <https://doi.org/10.1016/j.memsci.2013.11.036>
- Tsai JT, Su YS, Wang DM, Kuo JL, Lai JY, Deratani A (2010) Retainment of pore connectivity in membranes prepared with vapor-induced phase separation. *J Membrane Sci* 362(1–2):360–373. <https://doi.org/10.1016/j.memsci.2010.06.039>
- Venault A, Chang Y, Wu J, Wang D (2014) Influence of solvent composition and non-solvent activity on the crystalline morphology of PVDF membranes prepared by VIPS process and on their arising mechanical properties. *J Taiwan Inst Chem E* 45(3):1087–1097. <https://doi.org/10.1016/j.jtice.2013.08.014>
- Venault A, Chang K, Maggay IV, Chang Y (2023) Assessment of the DCMD performances of poly (vinylidene difluoride ) vapor-induced phase separation membranes with adjusted wettability via formation process parameter manipulation. *Desalination* 560:116682. <https://doi.org/10.1016/j.desal.2023.116682>
- Wang DL, Li K, Teo WK (2000) Porous PVDF asymmetric hollow fiber membranes prepared with the use of small molecular additives. *J Membrane Sci* 178(1–2):13–23. [https://doi.org/10.1016/S0376-7388\(00\)00460-9](https://doi.org/10.1016/S0376-7388(00)00460-9)
- Yao M, Tijing LD, Naidu G, Kim S, Matsuyama H, Fane AG, Shon HK (2020) A review of membrane wettability for the treatment of saline water deploying membrane distillation. *Desalination* 479:114312. <https://doi.org/10.1016/j.desal.2020.114312>
- Ye Q, Cheng L, Zhang L, Xing L, Chen H (2011) Preparation of symmetric network PVDF membranes for protein adsorption via vapor-induced phase separation. *J Macromol Sci B* 50(10):2004–2022. <https://doi.org/10.1080/00222348.2011.557606>
- Yushkin A, Balynin A, Efimov M, Pochivalov K, Petrova I, Volkov A (2022) Fabrication of polyacrylonitrile UF membranes by VIPS method with acetone as co-solvent. *Membranes* 12(5):523. <https://doi.org/10.3390/membranes12050523>
- Zhao Q, Xie R, Luo F, Faraj Y, Liu Z, Ju X, Wang W, Chu L (2018) Preparation of high strength poly (vinylidene fluoride ) porous membranes with cellular structure via vapor-induced phase separation. *J Membrane Sci* 549:151–164. <https://doi.org/10.1016/j.memsci.2017.10.068>